Design Considerations and Short-Circuit Characteristics of Fully Superconducting Wind Turbine Generators

Liu, Dong; Hasanov, Urfan; Ye, Changqing; Gou, Xiaofan; Wang, Xuezhou

DOI
10.1109/APPEEC48164.2020.9220445

Publication date
2020

Document Version
Accepted author manuscript

Published in
Proceedings of the 12th IEEE PES Asia-Pacific Power and Energy Engineering Conference, APPEEC 2020

Citation (APA)
Liu, D., Hasanov, U., Ye, C., Gou, X., & Wang, X. (2020). Design Considerations and Short-Circuit Characteristics of Fully Superconducting Wind Turbine Generators. In *Proceedings of the 12th IEEE PES Asia-Pacific Power and Energy Engineering Conference, APPEEC 2020* Article 9220445 IEEE. https://doi.org/10.1109/APPEEC48164.2020.9220445

Design Considerations and Short-Circuit Characteristics of Fully Superconducting Wind Turbine Generators

Dong Liu
College of Energy and Electrical Engineering
Hohai University
Nanjing, China
dongliu@hhu.edu.cn

Urfan Hasanov
College of Energy and Electrical Engineering
Hohai University
Nanjing, China
urfan98@gmail.com

Changqing Ye
College of Internet of Things
Hohai University
Changzhou, China
changqingye@hhu.edu.cn

Xiaofan Gou
College of Mechanics and Materials
Hohai University
Nanjing, China
xfgou@hhu.edu.cn

Xuezhou Wang
Faculty of Mechanical, Maritime and Materials Engineering
Delft University of Technology
Delft, Netherlands
x.wang-3@tudelft.nl

***Abstract*—Compared with partially superconducting generators, fully superconducting generators (F-SCGs) can further increase the torque density in large direct-drive wind turbine applications. Design trends of F-SCGs intend to increase the electrical loading by applying superconducting wires and boost the current density in the armature winding to meet the critical current density with a safety margin. High currents may cause a low power factor and require the power electronic converter to have a much larger capacity. In an F-SCG, furthermore, torques could be too high, and field and armature currents may exceed the critical currents during a generator short circuit. This paper studies the design of a 20 MW F-SCG with consideration of the control strategy and the power factor, and then evaluates the short circuit characteristic of the F-SCG. The results analysis shows that a capacitive load control should be adopted to avoid a significant drop in the power factor and to make full use of the current-carrying capability of superconductors. An $I_d = 0$ control can also be used with a medium current level. During the short circuit, the negative side is that the phase currents exceed the critical currents and cause quenches. The positive side is that the field currents stay below the critical currents and the torques do not exceed the mechanical limitation of three times the rated torque.**

Keywords— Fully superconducting generator, power factor, short circuit, superconducting armature, wind turbine

I. Introduction

Superconducting (SC) generators can be much more compact and lighter than the conventional permanent magnet (PM) counterparts. Partially superconducting generators (PSCGs) with the field winding being superconducting have been proposed for large direct-drive offshore wind turbines for years [1]-[4]. Fully SC generators (F-SCGs) which also make armature winding superconducting can further increase the torque density. The AC loss in the SC armature winding, as a critical problem for F-SCGs, is being reduced by implementing special wire architectures, such as multi-filamentary stranded cables with MgB_2 wires and Roebel cables with the 2nd-generation high-temperature superconducting (HTS) tapes [5]-[8]. As F-SCGs are becoming increasingly feasible, it is needed to consider the design methods or design philosophies which will achieve the desired performance.

The literature on designing F-SCGs has two trends. One is to focus on the armature winding design and try to estimate and lower the AC loss [5], [9], [10]. The other is to estimate the normal performance indicators, e.g. size, weight, cost, of the generator with the assumption that the AC loss is not a no-go factor [6], [11]-[13]. Both of the trends intend to increase the electrical loading by applying superconducting wires and boost the current density in the armature winding to meet the critical current density with a safety margin. Such a high current density may cause a low power factor and require the power electronic converter to have a much larger capacity. Finding a rated current for the armature winding to obtain a reasonable power factor will benefit the selection of the converter. However, it does not mean that the power factor is a key performance indicator for the design of an F-SCG since converters are nowadays cheap and a smaller and lighter generator could benefit more to the whole wind turbine.

An F-SCG usually avoids using magnetic iron for the field poles and the armature teeth to further reduce the weight since the main magnetic field has already been sufficiently high. The absence of iron reduces the reactance of the armature winding. Thus, the short circuit torque could be too high and needs an assessment. Moreover, both the field winding and the armature winding are superconducting. Their currents should stay under the critical currents during a generator short circuit and also need an assessment.

This paper studies the design of a 20 MW F-SCG with consideration of the control strategy and the power factor, and then evaluates the short circuit characteristics of an F-SCG design. The design study aims at revealing the relationship between the armature winding design and the power factor. The short circuit study aims at examining the phase current, field current and torque.

II. Basic Design of a 20 MW F-SCG

The F-SCG is designed for a 20 MW direct-drive wind turbine. The rated speed is 6.6 rpm and the rated voltage is 6.6 kV. The part about one pole of the generator is sketched in Fig. 1. The field winding on the rotor is made of ReBCO tapes operated at 30 K. The armature winding on the stator is made of multi-filamentary stranded MgB_2 cables operated at 20 K. Due to the different cryogenic temperatures, the rotor

This work is supported in part by the Natural Science Foundation of Jiangsu Province of China under Grant BK20190486, and in part by the Fundamental Research Funds for the Central Universities under Grant No. 2018B02114.

and the stator have separate cryostats. Either cryostat is cylindrical and accommodates the winding and its support structure. Magnetic iron is not used for the field pole and the armature teeth. The support structure of the field winding needs to both hold the winding in place, transfer the torque with shaft and isolate the heat. The support structure of the armature winding needs to hold the winding in place and connect the winding to a stationary frame. Back iron is still used in the rotor and the stator to confine the magnetic flux.

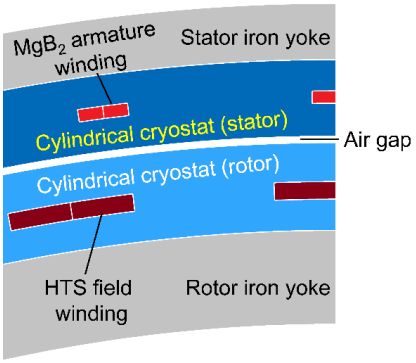

Fig. 1. Sketch of the part about one pole of the designed F-SCG

A. Operationg Point

Due to the absence of iron pole core, the rotor is non-salient and the generator can be controlled with the direct-axis current being zero, i.e. $I_d = 0$. With this control strategy, the power factor angle φ equals the power angle δ. Thus, this angle is determined by the voltage across the synchronous reactance XI if the excitation, i.e. $\dot{E}_p$, remains the same. A larger phase current $\dot{I}$ leads to a larger power factor angle φ and then a lower power factor cosφ. Therefore, a higher armature current can increase the torque density but also decrease the power factor. Both the $\dot{E}_p$ and terminal voltage $\dot{U}$ must be increased to keep the same power factor angle if the current remains this high.

Other control strategies include the control for a maximum torque per Ampere (MTPA) and the control for a unit power factor. In these control strategies, the current phasor $\dot{I}$ lies between $\dot{E}_p$ and $\dot{U}$ (capacitive load), in phase with $\dot{U}$ (unit power factor) or lags $\dot{U}$ (inductive load), as depicted in Fig.3. Keeping the same voltage level, the capacitive load control (Figs. 3a and 3b) can achieve a high armature current without significantly increasing the excitation $\dot{E}_p$. The angle between $\dot{E}_p$ and $\dot{U}$ can be tuned to achieve an MTPA. The levels of E_p and U can be similar. However, this control requires the converter to supply reactive power to the generator.

If the control for a unit power factor is used, as depicted in Fig. 3c, the excitation must be boosted and the power angle must be sufficiently large. However, a large power angle will reduce the static stability of the synchronous generator and a high no-load voltage is not desirable. Similarly, the inductive load control (Fig. 3d) also requires high excitation $\dot{E}_p$ but the generator supplies reactive power to the converter.

The capacitive load control is preferred for the concept of superconducting armature windings in which the current should be as high as the superconducting wire can safely carry. The $I_d = 0$ control can also be used when the armature current need not be that high or the superconducting wires have low current carrying capability. In the F-SCG design, MgB_2 is adopted in which the current carrying capability is highly limited by external magnetic fields. Therefore, the $I_d = 0$ control is chosen for this design. However, the power factor must be examined to maintain an acceptably high level.

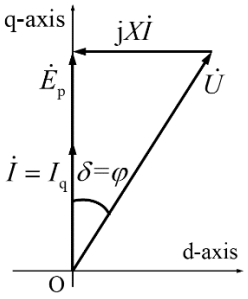

Fig. 2. Phasor diagram of zero direct-axis current control. The phase resistance is zero. $\dot{E}_p$ is the EMF, $\dot{U}$ is the phase voltage, $\dot{I}$ is the phase current, X is the synchronous reactance, δ is the power angle and φ is the power factor angle.

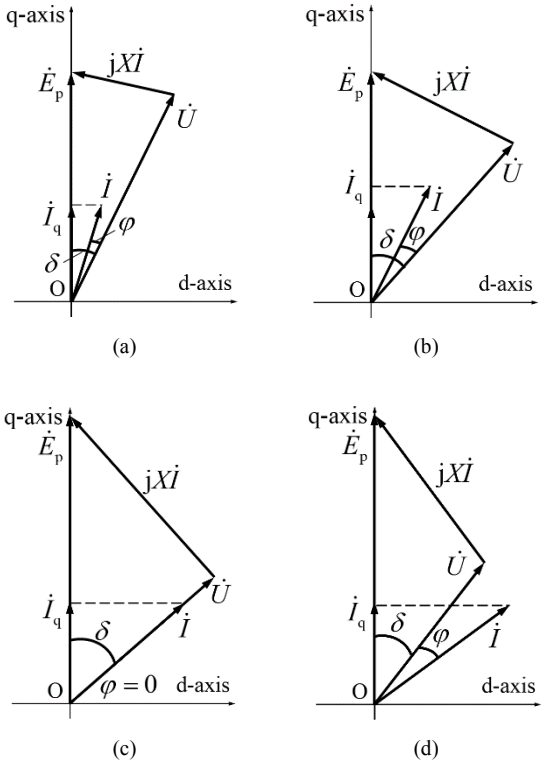

Fig. 3. Phasor diagrams of non-zero direct-axis current control. Note the RMS voltage U is kept constant. (a) Capacitive load, for a low current. (b) Capacitive load, for a high current. (c) Unit power factor, for a high current. (d) Inductive load, for a high current.

B. Armature winding type

The three-phase armature winding is a double-layer fractional-slot concentrated (DL-FSC) winding since tooth coils with racetrack shape avoid twisting at the end winding and the minimum bending radius of the MgB_2 cable can be satisfied. Single-layer racetrack coils can also form a winding with one slot per pole per phase, but the support structure is too complicated to realize [5]. Integral multiple slots per pole per phase cannot be applied since the end winding must be twisted and the wire is prone to breaking. Furthermore, fractional-slot concentrated windings result in a high leakage flux and can be used to reduce short circuit currents. However, this winding type has its drawbacks such as space harmonics. The slot-pole combination is chosen to be 0.4 slots per pole per phase which is mostly used in permanent magnet machines.

C. Pole pitch

Due to the large distance of 125 mm between the field winding and the armature winding, namely the magnetic air gap, the pole pitch should be large to reduce flux leakages. On the other hand, a too large pole pitch without iron core causes "M" shape flux under the pole. The induced no-load voltage will be an "M" shape too and the distortion will be too severe to be accepted. Therefore, the number of pole pairs is set to 20 and the resulting pole pitch is 427.3 mm to reach a stator bore diameter of 5.6 m. The distance from the field winding to the rotor iron yoke and the distance from the armature winding to the stator iron yoke are both 50 mm.

D. Field winding dimensioning

Since the pole pitch has been set, the remaining is to set the field coil dimension. One field coil consists of double pancakes of ReBCO tapes. Considering the fill factor of about 0.7, the coil height is fixed to 28 mm. The coil side width is varied to find an optimum point. Here the torque production is chosen as a criterion for this optimum point. The critical current of the field winding has little difference with the varied coil side width so the operating field current is kept the same as 144 A/mm^2. When increasing the coil side width, as shown in Fig. 4, the produced torque becomes saturated. The linear region stops at around 100-120 mm. For saving costs, the coil side width is set to 100 mm.

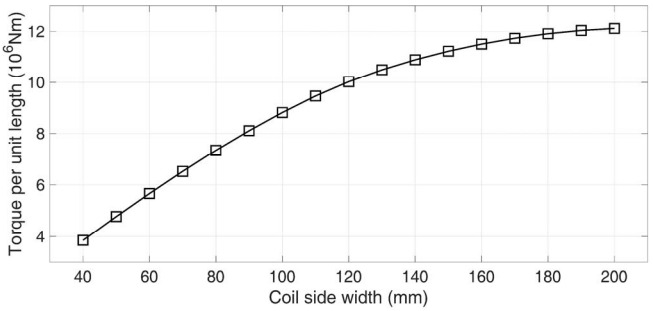

Fig. 4. Torque production per unit length with the field coil side width varied.

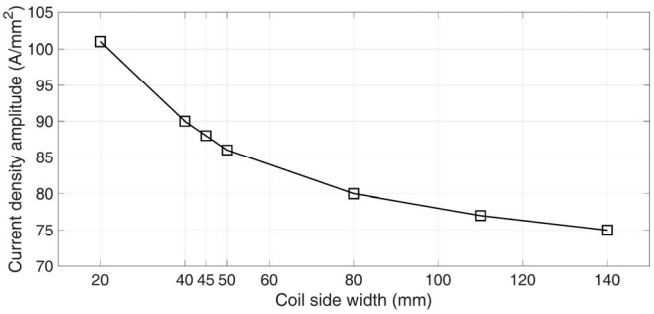

Fig. 5. Armature current amplitude with the armature coil side width varied.

III. Armature Winding Dimensioning and Power Factors

The armature winding adopts the stranded multifilamentary MgB_2 cables as described in [5]. The height of the MgB_2 racetrack coils is fixed to 20 mm and the width of the coil side is varied from 20 mm to 140 mm to find a value when the torque is sufficiently high while the power factor is acceptable. The field winding dimension is kept as 100 mm as found in Section II-D.

Unlike the field winding, the critical current of the armature winding significantly changes when varying the armature coil side width. Therefore, the operating current of the armature winding, i.e. the amplitude of the sinusoidal current, has the trend with respect to the coil side width as shown in Fig. 5. The current amplitude decreases when the coil side width increases. Importantly, the torque production increases the coil side width increases, as shown in Fig. 6. While a larger coil side benefits the torque production, it reduces the power factor drastically. As shown in Fig. 7, the width of 45 mm already reduces the power factor to lower than 0.85. If a power factor of 0.85 is required, the armature coil side width must be narrower than 40 mm.

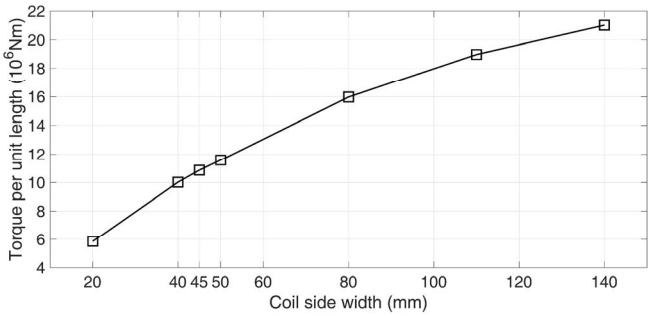

Fig. 6. Torque production per unit length with the armature coil side width varied.

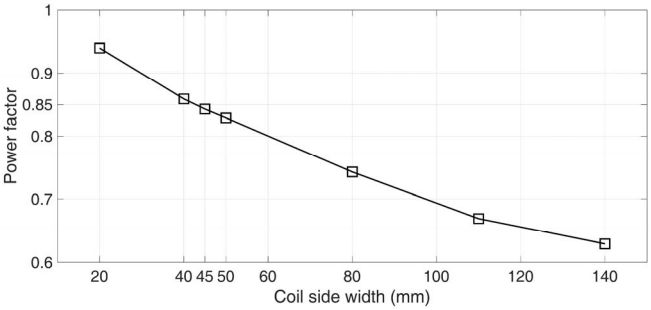

Fig. 7. Power factor with the armature coil side width varied.

TABLE I. Design Parameters of the F-SCG

Parameter	Value
Rated power	20 MW
Rated speed	6.6 rpm
Rated voltage	6.6 kV
Rated torque	31.8 MNm
Air gap diameter	5600 mm
Stack length	3615 mm
No. of pole pairs	20
No. of slots	48
No. of phases	3
HTS field coil height	28 mm
HTS field coil side width	100 mm
Armature coil height	20 mm
Armature coil side width	40 mm
Field yoke height	150 mm
Armature yoke height	90 mm
Distance from field winding to armature winding	125 mm
Distance from field coil to field yoke	50 mm
Distance from armature coil to armature yoke	50 mm
Rated armature current (amplitude)	3136 A/mm^2
Rated field current	346 A/mm^2
Power factor	0.859

Apparently, the power factor significantly limits the increase the coil size and then the torque production. If a high power factor is required, the coil side width can go to 140 mm

and even more, and the torque production can be boosted. However, as indicated in the phasor diagram in Fig. 2, the difference between E_p and U (both are the RMS values) will go much larger. The torque limitation due to the power factor could be solved by using different control strategies, such as the capacitive load control in Fig. 3a and the inductive load control in Fig. 3d.

IV. F-SCG Design Parameters

The generator design parameters are summarized in Table I . This design is based on the $I_d = 0$ control as shown in Fig. 2. Other control strategies will change the armature current phasor $\dot{I}$ and then change some of the design parameters related to the field winding dimensioning and the armature winding dimensioning. The resulting generator axial length will also be different.

V. Short Circuit Charachteristic

The F-SCG does not have iron in the field poles and the armature teeth, the inductance of the armature winding is thus low and short circuit currents can be high. However, the fractional-slot concentrated winding has a higher leakage inductance compared with integral-slot distributed windings. Such a high leakage may suppress the short circuit current and torque. Currents in the superconducting armature winding need to be examined in short circuits to check if the current exceeds the critical current and causes a quench. The torque must be examined to check if it exceeds the mechanical design limit which is usually three times the rated torque.

The field current must also be examined since the field winding is also superconducting and the current must stay lower than the critical current. Due to the large magnetic reluctance between the field winding and the armature winding, the mutual inductance between these windings is much lower than that in a fully ironed machine. This is an advantage to keep the field current below the critical current during a short circuit.

Since the superconducting armature winding carries high currents in normal operation, the magnetic energy stored in the generator is much higher than that in a partially superconducting generator. Thus, not only a no-load three-phase short circuit is considered but a rated-load short circuit should also be examined. A no-load three-phase and a rated-load three-phase short circuit are simulated with finite element methods using the field-circuit model [14]. The short circuit begins when the voltage of Phase A crosses zero. Five cycles from the start of the short circuit are simulated.

A. Armature currents

The currents of the three phases during the short circuit are plotted in Fig. 8 in per unit. The base current is 3136 A which the amplitude of the rated phase current. The critical current is also plotted, considering the maximum norm magnetic flux density in the armature winding. The negative parts of the phase currents are flipped over to the positive for comparison with the critical current.

Phase A has the maximum peak current since the short circuit begins when the flux linkage of Phase A is maximum. In all the three phases, the current exceeds the critical current in the first three cycles. Therefore, quenches are inevitable in the armature winding. The impact of the quenches is beyond the scope of this paper and will be studied in the future.

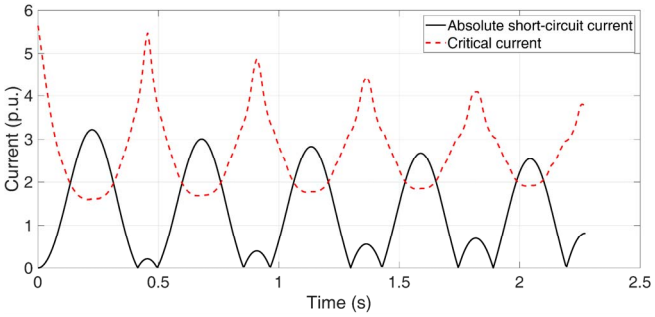

(a) Phase A, no-load

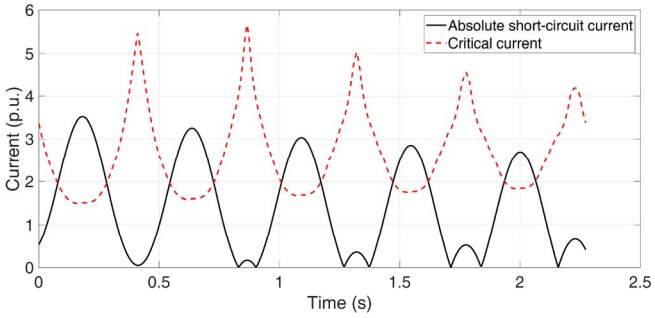

(b) Phase A, rated load

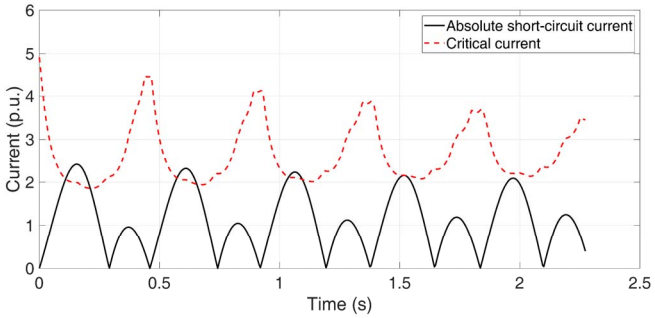

(c) Phase B, no-load

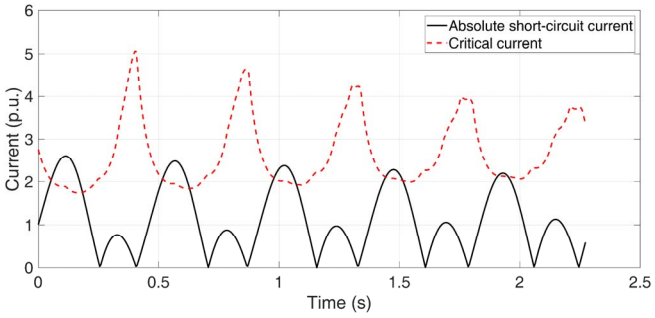

(d) Phase B, rated load

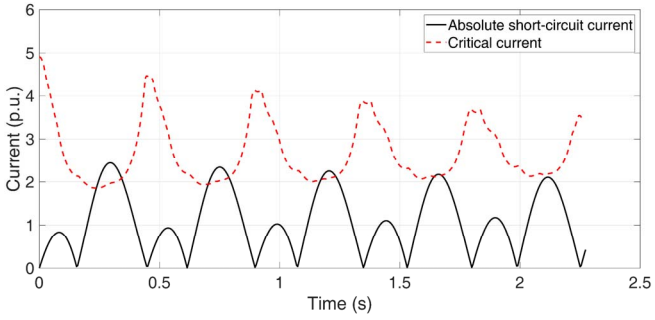

(e) Phase C, no-load

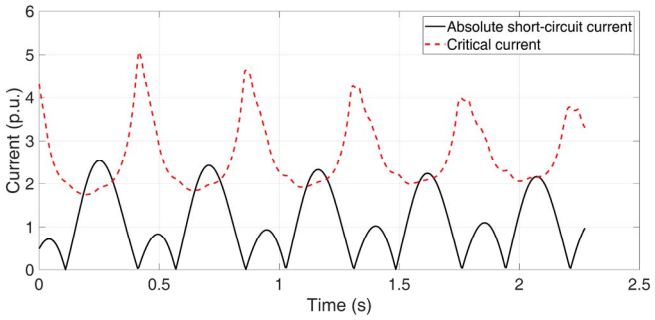

(f) Phase C, rated load

The rated load short circuit is not quite different from the no-load short circuit. The phase currents are slightly larger in the former case. This result indicates that the high current in the superconducting armature winding does not substantially boost the short circuit current.

B. *Field currents*

The currents of the field winding during the short circuit are plotted in Fig 9 in per unit. The base current is 346 A which the rated field current. The critical current is also plotted, considering the maximum norm magnetic flux density in the field winding. The rated load short circuit is not quite different from the no-load short circuit. In both cases, however, the field current does not exceed the critical current but stay lower than the critical current, although the first peak is close to the critical current. This result is due to that the non-ironed poles and teeth increase the reluctance and then mitigates the influence of the armature field on the field winding.

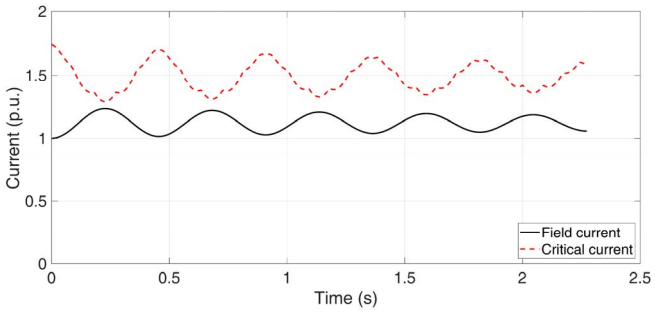

(a) No-load

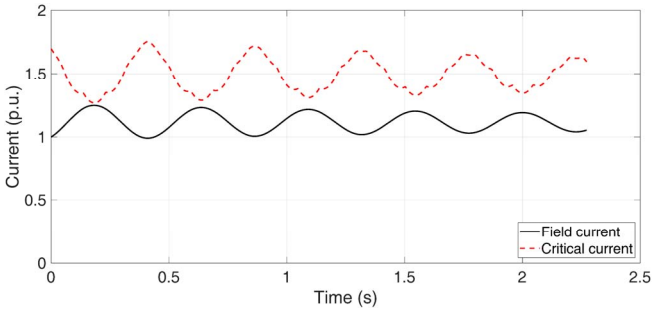

(b) Rated load

Fig. 9. Field currents during the no-load and rated-load three-phase short circuits, compared with the critical currents.

C. *Torque*

The electromagnetic torques produced during the short circuit are plotted in Fig 10 in per unit. The base torque is 31.8 MNm which is the rated torque. The rated load short circuit is not quite different from the no-load short circuit. In both cases, the peak torque does not exceed two times the rated torque. This result is due to that the fractional-slot concentrated winding has a large leakage inductance. Such a large leakage inductance suppresses the short circuit armature current and then the electromagnetic torque.

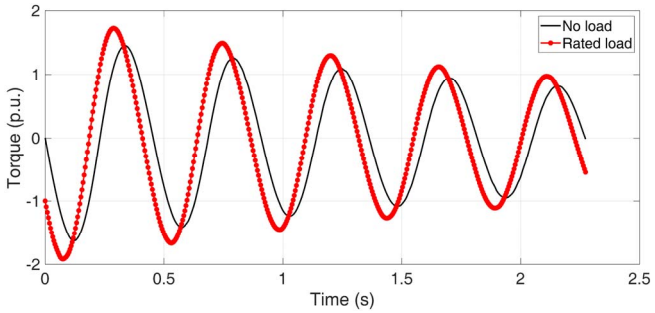

Fig. 10. Electromagnetic torque during the no-load and rated- load three-phase short circuits.

VI. Conclusions

This paper presents design considerations for a 20 MW direct-drive fully superconducting generator and then examines its short circuit characteristic. To make full use of the high current carrying capability in the superconducting armature winding, capacitive load control should be adopted to avoid a significant drop in the power factor. If the power factor is not required to be as high as 0.9, for example, the $I_d = 0$ control can also be used with a medium current level. The armature winding type is fractional-slot concentrated winding to make the end winding simple and avoid breaking due to bending.

A generator design with $I_d = 0$ control and power factor of 0.859 is presented, and its no-load and rated-load three-phase short circuits are simulated. During the short circuit, the phase currents exceed the critical currents and cause quench. The field currents stay below the critical currents, which is desired. The torques do not exceed the mechanical limitation of three times the rated torque, which is also a positive result. Since the capacitive load control has many advantages over the $I_d = 0$ control, especially the power factor issue, future work will take this control strategy, find the limits how high the armature current can reach and investigate other generator design philosophies.

References

[1] K. S. Haran et al., "High power density superconducting rotating machines -development status and technology roadmap," Supercond. Sci. and Techno., vol. 30, pp. 123002, 2017.

[2] B. B. Jensen, N. Mijatovic, and A. B. Abrahamsen, "Development of superconducting wind turbine generators," Journal of Renewable and Sustainable Energy, vol. 5, pp. 023137, 2013.

[3] H. Polinder, J. A. Ferreira, B. B. Jensen, A. B. Abrahamsen, K. Atallah, and R. a. McMahon, "Trends in wind turbine generator systems," IEEE J. Emerg. Sel. Top. Power Electron., vol. 1, pp. 174185, 2013.

[4] X. Song et al., "Designing and Basic Experimental Validation of the World's First MW-Class Direct-Drive Superconducting Wind Turbine Generator," IEEE Trans. Energy Convers., vol. 34, no. 4, pp. 22182225, Dec. 2019.

[5] S. S. Kalsi, "Superconducting Wind Turbine Generator Employing MgB2 Windings Both on Rotor and Stator," IEEE Trans. Appl. Supercond., vol. 24, no. 1, pp. 47-53, Feb. 2014, Art no. 5201907.

[6] T. Hoang, L. Quval, C. Berriaud and L. Vido, "Design of a 20- MW Fully Superconducting Wind Turbine Generator to Minimize the Levelized Cost of Energy," IEEE Trans. Appl. Supercond., vol. 28, no. 1, pp. 47-53, June 2018, Art no. 5206705.

[7] K. Suzuki et al., “Development of a laser scribing process of coated conductors for the reduction of AC losses,” Supercond. Sci. and Techno., vol. 20, no. 8, pp. 822826, 2007.

[8] W. Goldacker et al., “Roebel cables from REBCO coated conductors: a one-century-old concept for the superconductivity of the future,” Supercond. Sci. and Techno., vol. 27, pp. 1-16, 2014, Art no.093001.

[9] F. Xu, A. Chen, S. Yang, J. Cao, X. Liu and L. Li, “AC Loss Prediction in BSCCO-Tape Armature Winding Design of a Synchronous Motor,” IEEE Trans. Appl. Supercond., vol. 20, no. 3, pp. 1005-1008, June 2010.

[10] A. Kawagoe et al., “Numerical Analyses on the Influences of Armature Winding Shape and Yoke Arrangements on Total Losses in Fully Superconducting Synchronous Motors Using REBCO Tapes,” IEEE Trans. Appl. Supercond., vol. 22, no. 3, June 2018, Art no. 5208104.

[11] Y. Terao, M. Sekino and H. Ohsaki, “Electromagnetic Design of 10 MW Class Fully Superconducting Wind Turbine Generators,” IEEE Trans. Appl. Supercond., vol. 22, no. 3, June 2012, Art no. 5201904.

[12] X. Song, N. Mijatovic, B. B. Jensen and J. Holboll, “Design Study of Fully Superconducting Wind Turbine Generators,” IEEE Trans. Appl. Supercond., vol. 25, no. 3, June 2015, Art no. 5201907.

[13] S. Miura, M. Iwakuma and T. Izumi, “Lightweight Design of Tens-MW Fully-Superconducting Wind Turbine Generators With High-Performance REBa2Cu3Oy Wires,” IEEE Trans. Appl. Supercond., vol. 30, no. 4, Jun. 2020, Art. No. 5204106.

[14] X. Song et al., “Short circuit of a 10-MW high temperature superconducting wind turbine generator,” IEEE Trans. Appl. Supercond., vol. 27, no. 4, Jun. 2017, Art. No. 5201505.